ACS APPLIED MATERIALS & INTERFACES

Research Article

www.acsami.org

Pore Formation in a p-Type Silicon Wafer Using a Platinum Needle Electrode with Application of Square-Wave Potential Pulses in HF Solution

Tomohiko Sugita, Kazuki Hiramatsu, Shigeru Ikeda, and Michio Matsumura*

Research Center for Solar Energy Chemistry, Osaka University, 1-3 Machikaneyama, Toyonaka, Osaka 560-8531, Japan

Supporting Information

ABSTRACT: By bringing an anodically biased needle electrode into contact with n-type Si at its tip in a solution containing hydrofluoric acid, Si is etched at the interface with the needle electrode and a pore is formed. However, in the case of p-type Si, although pores can be formed, Si is likely to be corroded and covered with a microporous Si layer. This is due to injection of holes from the needle electrode into the bulk of p-type Si, which shifts its potential to a level more positive than the potential needed for corrosion and formation of a microporous Si layer. However, by applying square-wave potential pulses to a Pt needle electrode, these undesirable changes are prevented because holes injected into the bulk of Si during the period of anodic potential are annihilated with electrons injected into Si during the period of cathodic potential. Even under such conditions, holes supplied to the place near the Si/metal interface are used for etching p-type Si, leading to formation of a pore at the place where the Pt needle electrode was in contact.

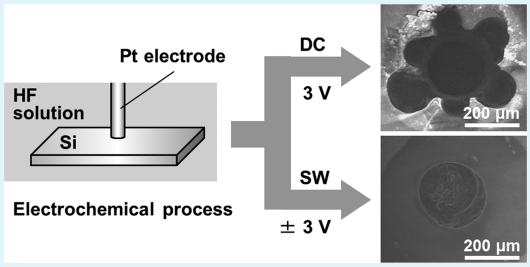

KEYWORDS: *silicon, pore formation, electrochemical etching, square-wave potential pulse*

INTRODUCTION

Wet etching of Si is widely used in the field of semiconductor processing. The processes are usually carried out in solutions containing nitric acid, hydrofluoric acid, and acetic acid. Among the components, nitric acid acts as a strong oxidant. Silicon oxidized by nitric acid dissolves in a solution containing HF, in which acetic acid acts as a buffer. Besides such conventional wet etching, a process called metal-assisted chemical etching (MACE),[1−11] in which hydrogen peroxide is normally used as the oxidant instead of nitric acid, has emerged recently. The metal particles loaded on Si catalyze electron transfer from Si to hydrogen peroxide. The metal particles also play a catalytic role in oxidizing Si at the metal/silicon interface. As a result, although hydrogen peroxide is a weaker oxidant than nitric acid, Si can be etched. The process is interesting because Si can be selectively etched at the site in direct contact with the metal particles. The mechanism is attributed to the dissolution of silicon oxide formed at the metal/Si interface[11] or sequential anodic dissolution of Si at the 3-phase interface of solution/metal/Si.[12] We proposed the latter mechanism on the basis of our results obtained using metal electrodes as below. Using site-selective etching of Si by MACE, pores,[1−11] nanowires,[13] and three-dimensional structures[14] are formed in Si. These structures may be used in new applications such as sensors,[15,16] micromachines,[17−19] and photonic devices.[20−22]

A process similar to MACE is possible by bringing an anodically biased metal electrode into contact with Si in a solution containing hydrogen peroxide.[12,23,24] The process is hereafter called electrochemical etching with a catalytic electrode (EECE), because the metal still plays catalytic role in oxidation of Si. A micromachining was achieved by bringing an anodically biased metal electrode into contact with Si in HF solution instead of metal particles.[12,23,24] Precious metals such as Pt, Ir, and Pd can be used as electrodes; their catalytic activity depends on the metals. An anodic potential is applied to the metal electrode which is also immersed in the HF solution, and Si is not connected to an external circuit except for the contact with the metal electrode. The advantage of EECE is that the position of the machining place and the rate of etching are easily controlled by adjusting the position and potential of the electrode. It is also interesting that any shapes such as grooves[23,24] and pores[12] can be formed in Si. We have succeeded in forming a pore with a diameter of 200 μm in an n-type Si wafer with a resistivity of 11 Ω cm at a rate of 2.9 μm min^{-1}.[12] Concerning electrochemical machining, a method, in which a workpiece is anodically polarized and a metal electrode (or a tool) is cathodically poralized, has been reported and applied to metals and Si.[25,26] EECE differs from this electrochemical machining in how the tool and workpiece are polarized, as mentioned above. Because EECE can be carried out without connecting a workpiece to an external circuit, the process is simpler than conventional electrochemical machining.

Received: October 12, 2012
Accepted: January 24, 2013
Published: January 24, 2013

   dx.doi.org/10.1021/am302314y | ACS Appl. Mater. Interfaces 2013, 5, 1262−1268

A problem with EECE as a method for machining Si is its difficulty in processing p-type Si.[12] When the potential applied to a Pt needle electrode was increased to a level higher than 2.5 V vs Ag/AgCl, the diameter of the pore formed in p-type Si became larger than the diameter of the needle electrode and a so-called microporous Si layer was formed all over the surface of the Si wafer. These undesirable changes for micromachining were due to injection of holes into the bulk of Si via the needle electrode. Once potential of p-type Si is shifted anodically to a certain level by the holes, Si is corroded or a microporous Si layer is formed on the surface.[27,28] It is therefore necessary to develop a method to process p-type Si wafers without harmful effects. Here we report a modification of EECE by applying square-wave potential pulses with a period of a few milliseconds to the needle electrode. The purpose is to remove holes injected excessively into the bulk of Si by applying a cathodic potential, which would enable processing of p-type Si by mitigating detrimental oxidation. Although different from our method, very precise electrochemical machining using square-wave potential pulses was proposed by Shuster et al.[25] They reported electrochemical micromachining of workpieces such as copper in an order of micrometers by modulating the potential applied between a fine electrode (or a tool) and a workpiece at a period of nanoseconds. Because formation of an electric double layer on the workpiece in such a short time is limited to a region very close to the electrode, anodic etching of the workpiece occurs only in a confined region, enabling very precise machining. In contrast, in EECE, the area of the machining is controlled by the area at which Si is in physical contact with the electrode. Another distinct difference between the two methods is that Si (or a workpiece) is not connected to a power source in EECE.

EXPERIMENTAL SECTION

Boron-doped (p-type) Si wafers with (100) crystallographic orientation and resistivity of 12 Ω cm were purchased from Shin-Etsu Chemical Co., Ltd. The Si wafers were cut into 1 × 1 cm^2 square pieces and used as test samples. A mirror-polished plane of the samples wafer was used for processing. Prior to the experiment, the samples were cleaned by immersing them in a mixture of hydrogen peroxide and sulfuric acid (30% H_2O_2:97% H_2SO_4 = 1:4 in volume) for 10 min, rinsing with ultrapure water (UPW) for 10 min, immersing in diluted HF solution (1% by weight) for 1 min, and rinsing again with UPW for 10 min. All of the chemicals used in this study were of reagent grade and used as-received. Platinum fine needles with a diameter of 200 μm, which were purchased from Nilaco Co., Ltd., were used for making pores in the Si wafers. The tips of these Pt needles were smoothed with emery papers and abrasives before usage.

The experimental setup for pore formation in Si wafers is shown in Figure 1. The process was performed with a standard electrochemical three-electrode system in 20 mol dm^{-3} HF solution without stirring at room temperature in the dark. Since hydrofluoric acid is a hazardous reagent, the experiments were carried out in a hood equipped with a scrubber. A Pt needle was used as a working electrode, a Pt foil was used as a counter electrode, and an Ag/AgCl electrode was used as a reference electrode. The Pt needle electrode was brought into contact at its tip with a Si sample in the HF solution using a holder made of Teflon, which gave a loading of 65 g onto the Pt needle during the processing. The length of the Pt needle extruding from the holder was about 1 mm. The potential of the Pt needle was controlled with a potentiostat (ALS Co., Ltd., 700C). Square-wave potential pulses were applied using the function-generator equipped in the potentiostat. Three types of square-waves used in this experiment are shown in Figure 2. Their high potential (V_H) was 3 V vs Ag/AgCl, their low potential (V_L) was −3 or 0 V vs Ag/AgCl, the duty ratio was always 1:1, and the cycle time (τ) was 2 or 6 ms. The morphologies of the

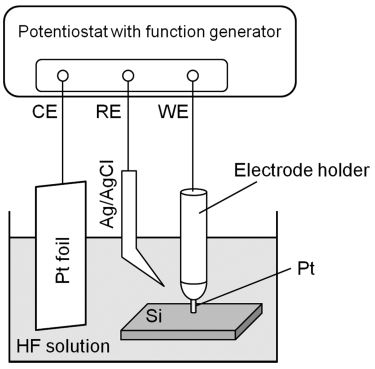

Figure 1. Setup of the electrochemical system for making a pore in Si.

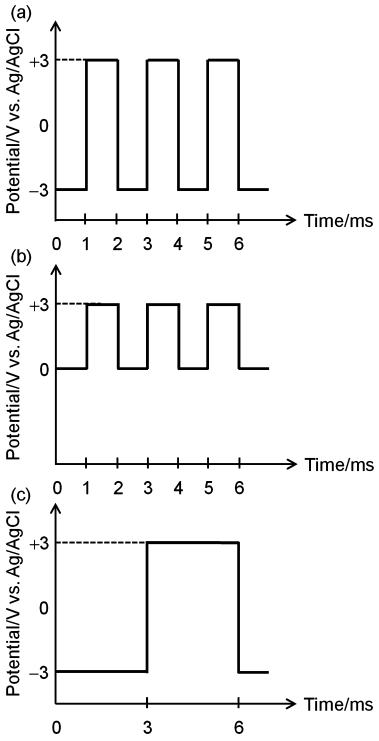

Figure 2. Three types of square-wave pulsed potentials applied to a Pt needle electrode: (a) ± 3 V vs Ag/AgCl, τ = 2 ms; (b) + 3 V/0 V vs Ag/AgCl, τ = 2 ms; and (c) ± 3 V vs Ag/AgCl, τ = 6 ms.

pores generated in Si by the processing were observed with a Hitachi S-5000 scanning electron microscope (SEM) after the process. The depth profiles of the pores were analyzed with a laser scanning microscope (KEYENCE Co., Ltd., VK−9700). For some experiments, the potential of the Si sample was controlled or monitored through an Al contact made on the backside.

RESULTS AND DISCUSSION

Generation of Pores in Si Wafers by Using a Pt Needle Electrode to Which DC or Square-Wave Potential Pulses Are Applied. Pores can be formed in Si by EECE using Pt, Ir or Pd needle electrodes to which an anodic DC potential is applied in HF solution.[12] The potential needed for pore formation depends on the kind of metal. By controlling the conditions of the potential and HF concentration, the diameter of the pore can be close to that of the needle electrode. With increase in potential, although the rate of pore formation increases, the diameter of the pore increases and the shape is deformed from a circular shape. This is especially true when p-

dx.doi.org/10.1021/am302314y | ACS Appl. Mater. Interfaces 2013, 5, 1262−1268

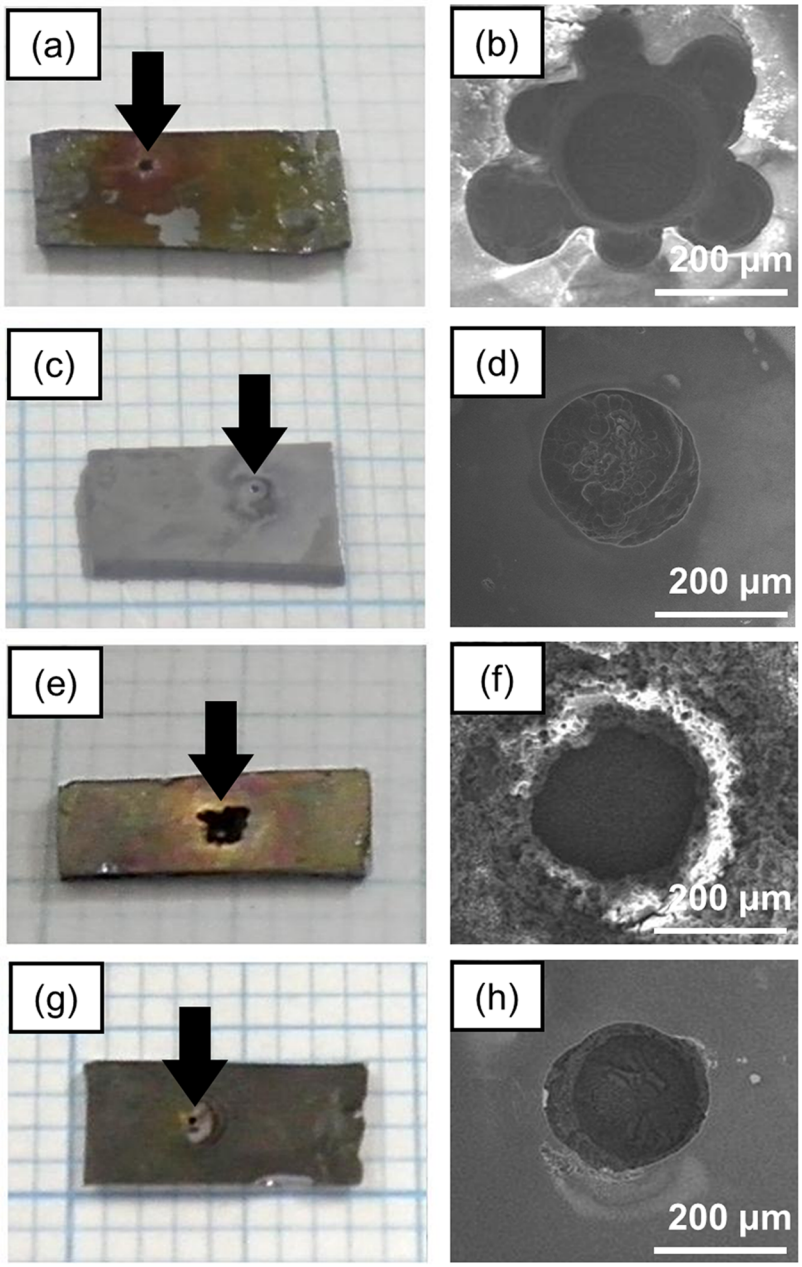

Figure 3. (a, c, e, g) Photomicrographs and (b, d, f, h) SEM images of Si samples after processing by using a Pt needle electrode with application of (a, b) DC + 3 V vs Ag/AgCl for 60 min, (c, d) square-wave potential pulses with V_H/V_L of ±3 V vs Ag/AgCl and τ of 2 ms for 120 min, (e, f) square-wave potential pulses with V_H/V_L of +3 V/0 V vs Ag/AgCl and τ of 2 ms for 120 min, and (g, h) square-wave potential pulses with V_H/V_L of ±3 V vs Ag/AgCl and τ of 6 ms for 120 min. b, d, f, and h show magnified images of pores formed in the corresponding samples. Pores in a, c, e, and g are shown by arrows.

type Si is processed. In addition, the surface of a p-type Si wafer after processing is roughened because of oxidation of Si and formation of a microporous Si layer. These changes occur also when a p-type Si electrode is anodically polarized in HF solution.[27,28]

In the present study, we used Pt as the needle electrode and studied pore formation in p-type Si (12 Ω cm). A typical pore formed in p-type Si after processing with a Pt needle electrode at a relatively high anodic potential (3 V vs Ag/AgCl) for 60 min and its magnified image are shown in Figures 3a and b, respectively. The depth of the pore was 360 μm; the pore formation rate was 6.0 μm min^{-1}. The area around the pore is corroded. The color of the entire surface of Si has changed and the surface has become matted. Figure 4a shows a cross sectional SEM image of the sample observed at a place about 2 mm from the pore, at which a microporous Si layer with a thickness of about 20 μm is formed. The corrosion and formation of a microporous silicon layer are caused by excessive injection of holes from the Pt needle electrode into the bulk of Si. Injection of too many holes and the undesirable morphological changes can be prevented by decreasing the potential below 2 V vs Ag/AgCl at a sacrifice of process rate.

To realize both reasonable process rate and good morphology of pores formed, we applied square-wave potential pulses to the Pt needle electrode instead of DC potential. When the potential was alternated between 3 V (V_H) and −3 V (V_L)

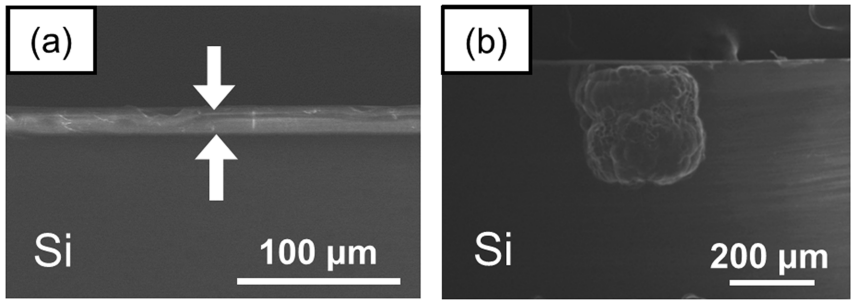

Figure 4. Cross-sectional SEM images of p-type Si samples after processing by using a Pt needle electrode with application of (a) DC + 3 V vs Ag/AgCl for 60 min and (b) square-wave potential pulses with V_H/V_L of ±3 V vs Ag/AgCl and τ of 2 ms for 120 min. The image for a was obtained at a place about 2 mm apart from the pore, where a microporous Si layer about 20 μm thick is formed on the surface.

vs Ag/AgCl with a cycle time (τ) of 2 ms (Figure 2a) for 120 min, a pore with a sharp edge was formed, as shown in Figure 3d. The diameter of the pore was about 240 μm, close to the diameter of the Pt wire (about 200 μm). As shown in Figure 4b, the wall of the pore was rugged to some extent and the depth of the pore was about 300 μm; the rate of pore formation was about 2.5 μm min^{-1}. Because pore formation hardly proceeds at a potential of −3 V vs Ag/AgCl, the etching rate in the period of 3 V vs Ag/AgCl is 5.0 μm min^{-1}, close to the rate obtained at the same potential by DC processing, i.e., 6 μm min^{-1}. Importantly, a microporous Si layer is not observed even at a place close to the pore (Figure 4b), and the color the Si sample did not change (Figure 3c). Hence, we found that the processing by EECE with square-wave potential pulses is useful to form a pore in p-type Si.

The morphology of the pore formed in Si and the surface condition of the wafer are dependent on V_H, V_L, and τ of the square-waves. When the sample was processed under the conditions of V_H = 3 V vs Ag/AgCl, V_L = 0 V vs Ag/AgCl, and τ = 2 ms (Figure 2b), Si was corroded around the pore, as shown in Figure 3e, f, and the surface was covered with a thick microporous Si layer (about 20 μm). This means that the potential of 0 V vs Ag/AgCl is not sufficiently negative to mitigate the corrosion and formation of a microporous Si layer. When the sample was processed under the conditions of V_H = 3 V vs Ag/AgCl, V_L = −3 V vs Ag/AgCl, and τ = 6 ms (Figure 2c), Si was slightly corroded around the pore, as shown in Figures 3g and h, and the surface of Si was covered with a microporous Si layer with a thickness of about 5 μm. This means that τ of 6 ms is too long to prevent the formation of a thick microporous Si layer. Figure 5 shows the relationship between τ and depth of pores formed by processing for 2 h at V_H = 3 V vs Ag/AgCl, V_L = −3 V vs Ag/AgCl. The pore formation rate becomes low at τ shorter than 2 ms. Results of the experiments under different conditions showed that the first conditions, i.e., V_H = 3 V vs Ag/AgCl, V_L = −3 V vs Ag/AgCl, and τ = 2 ms, are promising for the formation of pores in p-type Si with well-controlled shapes at a reasonable rate. The Pt needle electrode after processing under the conditions for 2 h did not show morphological change, although deposit was observed around the tip (see Figure S1 in the Supporting Information). Deposits were not observed when it was used for pore formation under the condition of DC potential of 3 V vs Ag/AgCl. We assume that products or intermediates of etching were electrochemically reduced and precipitated on the needle electrode during cathodic potential pulses.

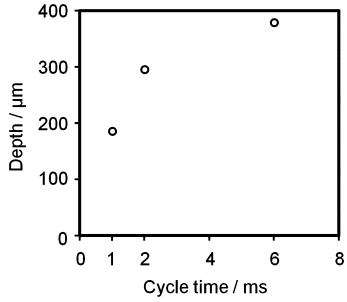

Figure 5. Dependence of depth of pores formed in Si samples on cycle time (τ) of square-wave potential pulses (V_H/V_L = ± 3 V vs Ag/AgCl) applied to a Pt needle electrode. Process time was 120 min.

Electrochemical Measurements to Explain the Effect of Square-Wave Potential Pulses Applied to a Pt Needle Electrode. To clarify the origin of the effect of the potential alternation, we monitored the currents flowing through the Pt needle electrode during the process of pore formation. Figure 6 shows the results for the above 3 potential-alternation modes: (a) V_H = 3 V, V_L = −3 V, τ = 2 ms, (b) V_H = 3 V, V_L = 0 V, τ = 2 ms, and (c) V_H = 3 V, V_L = −3 V, τ = 6 ms. The currents were measured by connecting the contact between the Pt needle electrode and the Si sample (solid lines) and disconnecting the contact (dotted lines). Currents were monitored after the current pattern had reached a steady state, about 30 min after starting the measurements. The important point is that a larger current flowed when the Pt needle electrode was in contact with the Si wafer. For the measurements, the sidewall of the Pt needle electrode was covered with a Teflon holder and grease (DAIKIN INDUSTRIES, Ltd., DAIFLOIL) so that the current at the Pt/solution interface became small.

The difference in the currents shown in Figures 6a−c is plotted in Figures 7a−c. When V_L is −3 V vs Ag/AgCl (Figure 6a, c), the cathodic current is much larger than that observed with V_L of 0 V vs Ag/AgCl (Figure 6b). This suggests that electrons are injected into Si at −3 V vs Ag/AgCl, but the injection is very small at 0 V vs Ag/AgCl. The patterns in Figures 7a and c show anodic current peaks with noticeable widths that appear when the potential is switched to V_H. These peaks are attributed to escape of electrons that have accumulated in the Si wafers while the potential was set at V_L. In the case of Figure 7c (τ = 6 ms), the current peaks appear at about 0.5 ms after the potential was switched to V_H. Although the details are not clear, we suspect that the conditions of the Pt/Si interface were changed and the potential barrier for the electron transfer across the interface was increased, while the potential was kept at −3 V vs Ag/AgCl

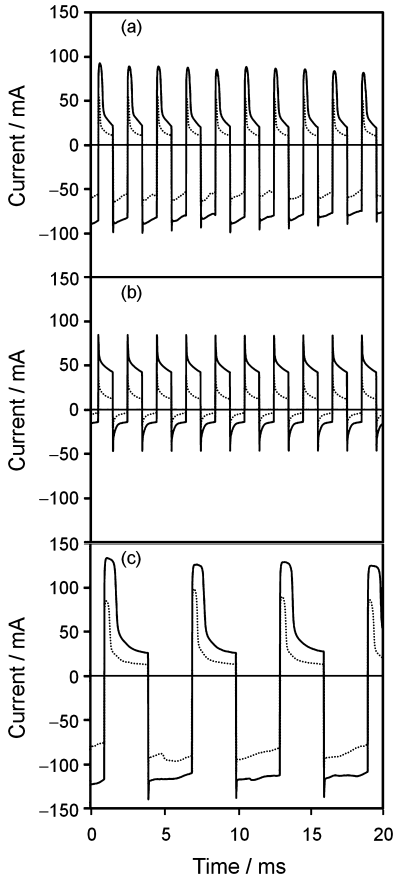

Figure 6. Currents flowing through a Pt needle electrode during the process of pore formation by application of square-wave potential pulses: (a) V_H/V_L of ±3 V vs Ag/AgCl, τ = 2 ms, (b) V_H/V_L of +3 V/0 V vs Ag/AgCl, τ = 2 ms, and (c) V_H/V_L of ±3 V vs Ag/AgCl, τ = 6 ms. The currents were measured by connecting the contact between the Pt needle electrode and the Si sample (solid lines) and disconnecting the contact (dotted lines).

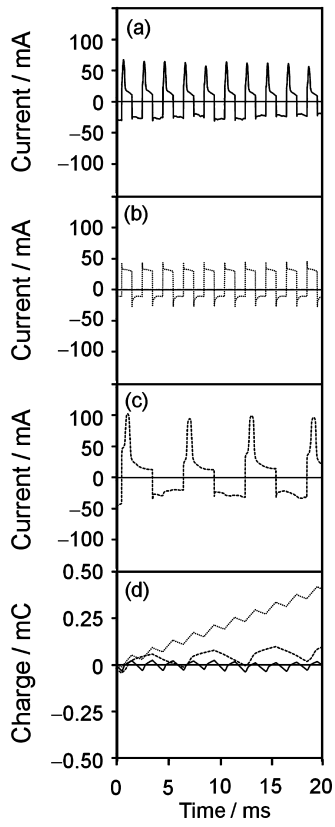

Figure 7. Currents flowing between the Pt needle electrode and Si during the process of pore formation by application of square-wave potential pulses of (a) V_H/V_L of ±3 V vs Ag/AgCl, τ = 2 ms, (b) V_H/V_L of +3 V/0 V vs Ag/AgCl, τ = 2 ms, and (c) V_H/V_L of ±3 V vs Ag/AgCl, τ = 6 ms, and (d) integration of the currents shown in (a)–(c). The currents were obtained from the results shown in Figures 6(a)–(c) by subtracting the currents shown by dotted lines from the currents shown by solid lines.

for 3 ms, and that it took about 0.5 ms for recovery to the original conditions after the potential had been switched to 3 V vs Ag/AgCl.

Figure 7d shows integration of the curves shown in Figures 7a–c from t = 0. When the potential was altered between ±3 V vs Ag/AgCl at τ of 2 ms, the integral curve (a solid line) fluctuated across the baseline and practically no net charge was transported across the Pt/Si interface over the period of 20 ms. This corresponds to the fact that, in Figure 7a, the anodic composition is nearly equal to the cathodic composition in each cycle. However, a certain amount of positive charge must be used for making a pore in Si. The charge necessary for formation of a pore with a depth of 300 μm and a diameter of 200 μm, which is close to the morphology of the pore formed after processing for 120 min, is about 0.3 C based on the assumption that Si dissolves in HF solution by

$$Si + 6HF + 4h^+ \rightarrow SiF_6^{2-} + 6H^+ \quad (1)$$

where h^+ is the hole injected into Si from the Pt electrode. Hence, the average current used for pore formation is 0.042 mA and the charge for 20 ms is about 0.83 μC, which is negligibly small on the scale used for Figure 7d. Therefore, the current shown in Figure 7a is assigned to transfer of electrons and holes to and from Pt across the Pt/Si interface, with very small number of holes being used for pore formation. The process can also be regarded mostly as charging and discharging at the electrical double layer formed at the Si/electrolyte interface. When τ is increased to 6 ms, the integral curve (a broken line) tends to increase with time at an average current of 3.6 mA (0.071 mC over 20 ms). This current is much higher than the current needed for making a pore in Si under the same condition, i.e., about 0.053 mA. Most of the excessive charges are expected to be used for making the microporous Si layer over the wafer surface. The microporous Si layer is formed during the period of V_H of 3 V vs Ag/AgCl in which an excessive number of holes are injected into the Si sample, which shift potential of Si to a level positive enough to drive the microporous Si layer formation and corrosion of Si using the holes supplied from the Pt electrode. On the other hand, when τ is 2 ms, because the charging and discharging at the electrical double layer formed at the Si/electrolyte interface is limited due to the short period, the potential difference generated across the Si/electrolyte interface is not large enough to induce electrochemical reactions of Si. Hence, the injected holes are mostly used to annihilate electrons injected from the Pt electrode during the V_L period and to make a pore in Si.

When V_L is set at 0 V vs Ag/AgCl, the integral curve (dotted line in Figure 7d) keeps increasing even at τ of 2 ms. The slope of increase corresponds to 19 mA (0.38 mC over 20 ms), which should be related to the conspicuous corrosion of Si and the formation of a thick microporous Si layer. These phenomena

are attributed to the fact that V_L of 0 V vs Ag/AgCl is not low enough to inject electrons from the Pt electrode into Si, which is needed to annihilate excessive holes injected during the V_H period, as will be discussed later.

To correlate the results obtained by the above-measurements with the electrochemical behavior of Si, we studied the electrochemical properties of the p-type Si substrate in HF solution. Figure 8 shows the potential−current behavior of a p-type Si substrate in HF solution, which was measured using the Si sample as the working electrode; the potential was controlled through the back contact. A remarkable anodic current was observed at potentials more anodic than 0 V vs Ag/AgCl. The anodic current leads to formation of a microporous Si layer and/or electrochemical etching of Si, which depends on the current density and HF concentration.[27,28] On the other hand, a cathodic current was hardly observed at potentials more positive than about −2 V vs Ag/AgCl because a depletion layer was formed near the interface with HF solution. At a potential of −3 V vs Ag/AgCl, where an inversion layer is formed at the interface, a small current due to hydrogen production or reduction of oxygen is observed.

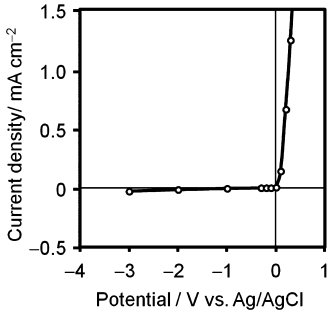

Figure 8. Current density−potential curve of a p-type Si (12 Ω cm) electrode measured in 20 mol dm^{-3} HF solution.

We then measured potentials of the p-type Si substrates, which was in contact with the Pt needle electrode. The potential of the Si sample was monitored through the back contact. Figure 9 shows the potential of the Si sample that was in contact with the Pt electrode, to which different potentials were applied. After reaching an equilibrium state under an open-circuit condition, at which the potential of the Si wafer was in the range of −0.1 to −0.2 V vs Ag/AgCl, a potential was externally applied to the Pt electrode and change in the potential of the Si wafer was monitored. When 3 V vs Ag/AgCl was applied to the Pt electrode, the potential of the Si wafer shifted to about 0.1 V vs Ag/AgCl as shown in Figure 9a; the change in the potential was about 0.2 to 0.3 V. When 0 V vs Ag/AgCl was applied to the Pt electrode, only a very small change in the potential was observed as shown in Figure 9b. In contrast to these cases, when −3 V vs Ag/AgCl was applied to the Pt electrode, the potential of the Si wafer shifted greatly to about −2.7 to −2.5 V vs Ag/AgCl, as shown in Figure 9c. This large negative shift of the potential suggests that electrons accumulate in the Si wafer because of the poor catalytic activity of Si for hydrogen evolution and band bending in p-type Si near the Si/electrolyte interface. Although the positive shift of about 0.2 to 0.3 V, which was observed when the Pt electrode was biased to 3 V vs Ag/AgCl, is small, this means that holes do not accumulate in Si but are easily consumed by the anodic process if potential of the Si wafer becomes more positive than 0 V vs Ag/AgCl, which is seen as an anodic current in Figure 8.

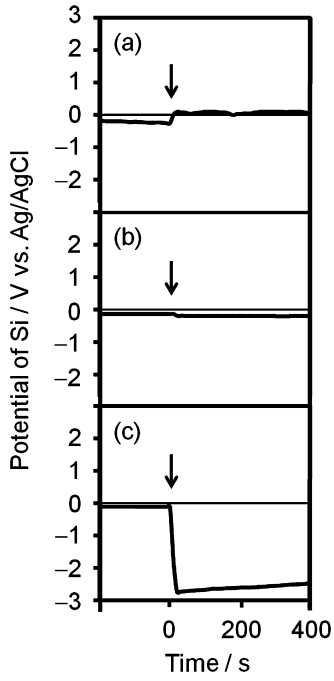

Figure 9. Change in potential of a p-type Si (12 Ω cm) substrate in contact with a Pt needle electrode by application of potential to the Pt needle electrode in 20 mol dm^{-3} HF solution: (a) 3 V vs Ag/AgCl, (b) 0 V vs Ag/AgCl, and (c) − 3 V vs Ag/AgCl. Arrows show the time when potentials were applied after reaching an equilibrium state under an open-circuit condition.

Hence, it is very important to prevent accumulation of holes in p-type Si to avoid corrosion and formation of a microporous Si layer. Application of square-wave potential pulses to the needle electrode is effective for the prevention. Although there may be other possibilities, we consider that the conditions of V_H = 3 V, V_L = −3 V, and τ = 2 ms are useful to meet the requirement and also to allow pore formation at a reasonable speed in p-type Si by using a Pt needle electrode. It should be noted that appropriate τ to prevent formation of a microporous Si layer and corrosion of Si must be dependent on the kind of metal used as an electrode. This is because τ is determined by the rate of carrier injection from the electrode into Si but not by drift of carriers in Si.

CONCLUSIONS

By applying square-wave potential pulses to a Pt needle electrode that is in contact with a p-type Si wafer in HF solution, alternated anodic and cathodic currents were observed, and they are attributed to the injection of holes and electrons into the bulk of the Si wafer. Under optimized conditions, holes are annihilated by electrons, which are respectively injected under anodic and cathodic conditions. However, the etching of Si occurs mostly at the site of Si/metal contact. As a result, pores can be formed in Si substrates at a reasonably high rate with little corrosion of Si or formation of microporous Si layers. We expect this electrochemical method to be applicable not only to making pores in Si but also to micromachining Si by accurately shifting the position of the electrode during processing.

■ ASSOCIATED CONTENT

Supporting Information

Photomicrographs of Pt needle electrodes after processing p-type Si; photomigcrographs of Pt needle electrodes after processing p-type Si with application of (a) DC + 3 V vs Ag/AgCl for 60 min and (b) square-wave potential pulses with V_H/V_L of ±3 V vs Ag/AgCl and τ of 2 ms for 120 min. This material is available free of charge via the Internet at http://pubs.acs.org.

■ AUTHOR INFORMATION

Corresponding Author

*E-mail: matsu@chem.es.osaka-u.ac.jp.

Notes

The authors declare no competing financial interest.

■ ACKNOWLEDGMENTS

This work was supported by a Grant-in-Aid for Scientific Research on Fundamental Research (24656232) from the Ministry of Education, Culture, Sports, Science and Technology, Japan. T.S. expresses his special thanks for the Global COE (center of excellence) Program "Global Education and Research Center for Bio-Environmental Chemistry" of Osaka University.

■ REFERENCES

(1) Li, X.; Bohn, P. W. *Appl. Phys. Lett.* **2000**, *77*, 2572.
(2) Tsujino, K.; Matsumura, M. *Adv. Mater.* **2005**, *17*, 1045.
(3) Tsujino, K.; Matsumura, M. *Electrochim. Acta* **2007**, *53*, 28.
(4) Lee, C.-L.; Tsujino, K.; Kanda, Y.; Ikeda, S.; Matsumura, M. *J. Mater. Chem.* **2008**, *18*, 1015.
(5) Huang, Z.; Geyer, N.; Werner, P.; de Boor, J.; Gösele, U. *Adv. Mater.* **2011**, *23*, 285.
(6) Peng, K.; Yan, Y. J.; Gao, S. P.; Zhu, J. *Adv. Mater.* **2002**, *14*, 1164.
(7) Peng, K.; Wu, Y.; Fan, H.; Zhong, X.; Xu, Y.; Zhu, J. *Angew. Chem., Int. Ed.* **2005**, *44*, 2733.
(8) Huang, Z.; Zhang, X.; Reiche, M.; Liu, L.; Lee, W.; Shimizu, T.; Senz, S.; Gösele, U. *Nano Lett.* **2008**, *8*, 3046.
(9) Fan, H.; Li, X.; Song, S.; Xu, Y.; Zhu, J. *Nanotechnology* **2008**, *19*, 255703.
(10) Peng, K.; Jie, J.; Zhang, W.; Lee, S. T. *Appl. Phys. Lett.* **2008**, *93*, 033105.
(11) Chartier, C.; Bastide, S.; Lévy-Clément, C. *Electrochem. Acta.* **2008**, *53*, 5509.
(12) Sugita, T.; Lee, C.-L.; Ikeda, S.; Matsumura, M. *ACS Appl. Mater. Interfaces* **2011**, *3*, 2417.
(13) Peng, K.; Fang, H.; Hu, J.; Wu, Y.; Zhu, J.; Yan, Y.; Lee, S. T. *Chem.—Eur. J.* **2006**, *12*, 7942.
(14) Rykaczewski, K.; Hildreth, O. J.; Wong, C. P.; Fedorov, A. G.; Scott, J. H. J. *Nano Lett.* **2011**, *11*, 2369.
(15) Cui, Y.; Wei, Q.; Park, H.; Lieber, C. M. *Science* **2001**, *293*, 1289.
(16) Patolsky, F.; Zheng, G.; Lieber, C. M. *Nat. Protoc.* **2006**, *1*, 1711.
(17) Ottow, S.; Lehmann, V.; Föll, H. *Appl. Phys. A: Mater. Sci. Process* **1996**, *63*, 153.
(18) Lang, W. *Mater. Sci. Eng., R* **1996**, *17*, 1.
(19) Judy, J. W. *Smart Mater. Struct.* **2001**, *10*, 1115.
(20) Grüning, U.; Lehmann, V.; Engelhardt, C. M. *Appl. Phys. Lett.* **1995**, *66*, 3254.
(21) Bettotti, P.; Dal Negro, L.; Gaburro, Z.; Pavesi, L.; Lui, A.; Galli, M.; Patrini, M.; Marabelli, F. *J. Appl. Phys.* **2002**, *92*, 6966.
(22) Wehrspohn, R. B.; Schilling, J. *Phys. Stat. Sol. A* **2003**, *197*, 673.
(23) Lee, C.-L.; Tsujino, K.; Kanda, Y.; Hirai, T.; Ikeda, S.; Matsumura, M. *J. Electrochem. Soc.* **2009**, *156*, H134.
(24) Salem, M. S.; Lee, C.-L.; Tsujino, K.; Ikeda, S.; Matsumura, M. *J. Mater. Process. Technol.* **2010**, *210*, 330.
(25) Schuster, R.; Kirchner, V.; Allongue, P.; Ertl, G. *Science* **2000**, *289*, 98.
(26) Allongue, P.; Jiang, P.; Kirchner, V.; Trimmer, A. L.; Schuster, R. J. *Phys. Chem. B* **2004**, *108*, 14434.
(27) Lehmann, V. *Electrochemistry of Silicon*; Wiley-VCH: Weinheim, Germany, 2002.
(28) Lehmann, V.; Stengl, R.; Luigart, A. *Mater. Sci. Eng., B* **2000**, *69*, 11.